HUMAN GENE THERAPY 23:951–959 (September 2012)

DOI: 10.1089/hum.2012.047

Characterization of Infectivity-Enhanced Conditionally Replicating Adenovectors for Prostate Cancer Radiovirotherapy

Michael J. Oneal,[1] Miguel A. Trujillo,[2] Julia Davydova,[3] Samantha McDonough,[2] Masato Yamamoto,[3] and John C. Morris III[2]

Abstract

Prostate cancer (PCa) is the second most commonly diagnosed and sixth leading cause of cancer death in American men and one for which no curative therapy exists after metastasis. To meet this need for novel therapies, our laboratory has previously generated conditionally replicating adenovirus (CRAd) vectors expressing the sodium iodide symporter (hNIS). This virus transduced PCa cells and induced functional NIS expression, allowing for noninvasive tumor imaging and combination therapy with radioiodide, referred to as radiovirotherapy. We have now generated two new modified vectors to further improve efficacy. Ad5/3PB-ADP-hNIS and Ad5/3PB-hNIS include a hybrid Ad5/3 fiber knob to improve transduction efficiency, and express NIS from the endogenous major late promoter to restrict NIS expression to target cells. Additionally, Ad5/3PB-ADP-hNIS includes the adenovirus death protein (ADP), which hastens the release of viral particles after assembly. These two vectors specifically induce radioisotope uptake, cytopathic effect, and viral replication in androgen receptor–expressing PCa cell lines with Ad5/3PB-ADP-hNIS showing earlier ^{131}I uptake and cytolysis at low multiplicity of infection. SPECT-CT imaging of xenograft tumors infected with Ad5/3PB-hNIS showed steady uptake, whereas infection with Ad5/3PB-ADP-hNIS led to increasing uptake, indicating viral spread. Radiovirotherapy of xenograft LNCaP tumors with Ad5/3PB-ADP-hNIS showed the most significant survival extension versus control tumors ($p = 0.001$), but the benefit of radiovirotherapy was not statistically significant compared with virotherapy alone in this model. These results show the potential of Ad5/3PB-ADP-hNIS as a vector for treatment of prostate cancer.

Introduction

As the second most frequently diagnosed cancer and sixth most frequent cause of cancer death in men worldwide (Jemal *et al.*, 2011), there is a need for novel and effective prostate cancer (PCa) treatments. Although androgen-deprivation therapy (Mottet *et al.*, 2011) and radical prostatectomy (Hugosson *et al.*, 2011) extend survival of PCa patients, the prognosis remains poor for metastatic or androgen-resistant cancer (Tannock *et al.*, 2004; Scosyrev *et al.*, 2011). These recurrences after treatment speak to the heterogeneity of cancer as a disease, where single-therapy treatment does not account for the variety of adaptive mutations present in a cancer cell population. As such, a multimodal therapy will likely be required for successful cancer treatment (Hanahan and Weinberg, 2011).

Our prior work has explored the use of adenovirus (Ad) vectors expressing the sodium iodide symporter (NIS) as just such a multimodal treatment. NIS has been exploited for decades to treat differentiated thyroid cancer (Luster *et al.*, 2008) using imaging isotopes such as ^{123}I or ^{124}I to noninvasively locate metastatic tumors, as well as radiotherapy via ^{131}I administration. The NIS transgene has been functionally expressed in a variety of cell types as a means to extend radioiodide treatment to nonthyroid cancers (Mandell *et al.*, 1999; Cho *et al.*, 2000; Spitzweg *et al.*, 2001; Kakinuma *et al.*, 2003; Dwyer *et al.*, 2005) and to noninvasively monitor viral replication and gene expression. This has led to

[1]Department of Molecular Medicine, Mayo Clinic, Rochester, MN 55904.
[2]Division of Endocrinology, Mayo Clinic, Rochester, MN 55904.
[3]Department of Surgery, University of Minnesota, Minneapolis, MN 55455.

investigation of the clinical utility of NIS-expressing vectors [Barton *et al*., 2008; Davis, 2011 (ongoing); Galanis, 2011 (ongoing)].

Conditionally replicating adenoviral (CRAd) vectors expressing high levels of NIS can combine ^{131}I radiotherapy with oncolytic virotherapy, achieving the goal of multimodal treatment and circumventing the problem of low transduction efficiency observed in gene-therapy trials thus far (Waehler *et al*., 2007; Trujillo *et al*., 2009, 2010). Our first CRAd, Ad5PB-RSV-hNIS, regulated E1a expression by the androgen-responsive promoter element ARR2PB (Zhang *et al*., 2000) and expressed NIS from the strong, nonspecific rous sarcoma virus (RSV) promoter. Viral replication was restricted to PCa cells, where androgen receptor (AR) is often overexpressed (Linja *et al*., 2001; Edwards *et al*., 2003) and resulted in tumor-specific cytolysis. Ad5PB-RSV-NIS significantly extended the survival time of radiovirotherapy-treated LNCaP-xenografted mice, demonstrating the potential of this approach.

We have now examined other improvements to vector design and describe two such vectors in this report. Ad5/3PB-ADP-hNIS and Ad5/3PB-hNIS control E1 expression through the probasin (PB) promoter, and NIS expression through the endogenous Ad major late promoter (MLP). The MLP is fully activated subsequent to E1 expression (Tribouley *et al*., 1994; Lutz and Kedinger, 1996) and can robustly express E3 transgenes (Ono *et al*., 2005; Davydova *et al*., 2010). Placing NIS under the control of a promoter downstream of E1 ties NIS expression to viral replication and increases its utility as a marker of replication. Also, the fiber knob protein has been modified to improve infectivity. Coxsackie adenovirus receptor (CAR) expression is often down-regulated or absent in late-stage PCa as tissue architecture becomes more disrupted (Rauen *et al*., 2002; Dash *et al*., 2010; Kuster *et al*., 2010), limiting infectivity by Ad5 vectors. Reduced CAR expression has been addressed by the use of modified fiber proteins containing the knob domain of Ad serotype 3, which binds to desmoglein-2 (DSG-2) (Wang *et al*., 2011). Increased DSG-2 expression has been observed in prostate cell lines with high metastatic potential, making it a logical target for mediating viral entry (Trojan *et al*., 2005). Finally, we reinserted an E3 protein removed from our previous CRAd, the adenovirus death protein (ADP). ADP mediates cell lysis after viral assembly is complete, greatly increasing the rate of viral spread (Tollefson *et al*., 1996). Overexpression of ADP has been used (Doronin *et al*., 2003) to compensate for low initial tumor transduction rates, a central problem of virotherapy. This quicker spread has also led to enhanced transgene expression under low multiplicity-of-infection (MOI) conditions (Davydova *et al*., 2010). By increasing viral spread in an NIS-expressing vector, it may be possible to increase the number of cells available to take up radioisotope, and the total tumor uptake as a consequence. However, because the increased rate of cell membrane disruption may also negatively impact radioiodide uptake, we wished to examine the contributions of increased cytolysis to radioiodide uptake and therapy in this model.

In this report, we describe Ad5/3PB-ADP-hNIS and Ad5/3PB-hNIS, Ad5-based vectors containing the modifications described above and differing only in ADP expression. Their specificity for AR-expressing cells, their *in vivo* efficacy for radioisotope uptake, and survival extension are characterized and compared with our previous work with Ad5PB-RSV-hNIS.

Materials and Methods

Cell lines

The PCa cell lines LNCaP, C4-2 (AR-positive), and PC-3 (AR-negative) were cultured as described (Spitzweg *et al*., 2001; Qu *et al*., 2004). All cells were kept at 37°C, 5% CO_2 during culture and assays. HEK 293A cells used in plaque assays were cultured as described above. *In vitro* assays were conducted on standard tissue culture plates except for assays using C4-2, which were conducted on collagen-I–coated plates.

Construction of the viral vectors

NIS was inserted into the E3 region as described (Davydova *et al*., 2010), with two exceptions. First, NIS was amplified by PCR amplification from pcDNA3_hNIS using primers containing a 5′ *Xba*I site and a 3′ *Sal*I site. After sequence fidelity was confirmed, *Xba*I/*Sal*I-digested gene product was ligated into *Xba*I/*Sal*I-restricted pShuttleΔE3ADPKanF2 or pShuttleΔE3KanF2 vector. Second, *Pme*I-linearized shuttle vector was homologously recombined to the backbone plasmid pMG553, which contains the chimeric fiber gene encoding the knob domain of Ad3 (Davydova *et al*., 2004), generating the backbone vectors for the wild-type E1 vectors Ad5/3-ADP-hNIS and Ad5/3-hNIS. Prostate-specific versions of these constructs were generated as described (Yamamoto *et al*., 2003) after the cyclooxygenase-2 (COX-2) promoter of the pShuttleCox-2LE1F vector was removed and the ARR_2PB composite PB promoter was inserted by blunt-end ligation. The purified Ad5/3PB-ADP-hNIS and Ad5/3PB-hNIS stocks were quantified at 6×10^{10} and 3×10^{10} vp/mL, respectively. Ratios of viral particles (vp) to plaque formation units (pfu) for both Ad5/3PB-ADP-hNIS and Ad5/3PB-hNIS were ~30 vp/pfu. No wild-type E1 virions were detected by quantitative PCR (QPCR). Purified virions were also confirmed by QPCR to contain the PB promoter, 5/3 hybrid fiber, and ADP genes. The construction of the Ad5PB-RSV-NIS vector has been previously described (Trujillo *et al*., 2010).

MTS assays of cytopathic effect

Cells (5,000 per well) were seeded in 96-well tissue culture plates and infected at the indicated MOI 24 hr later with a final medium volume of 200 μL. At the indicated time points, 50 μL of CellTiter 96 Aqueous One Solution Cell Proliferation Assay (Promega Corporation, Madison, WI) was added to each well and incubated at 37°C, 5%CO_2 for 2 hr. After incubation, absorbance at 490 nm was recorded using a Multiskan EX plate spectrophotometer (Thermo Electron Corporation, Waltham MA).

Crystal violet staining assays of cytopathic effect

Cells (50,000 per well) were seeded in 24-well tissue culture plates and infected 24 hr later at the indicated MOI. Seven days post infection, culture medium was removed and cells were incubated in 10% formalin for 5 min. Formalin was aspirated and cells were incubated at room temperature in 1% crystal violet in 10% methanol for 20 min. Cells were then

rinsed twice with distilled water and photographed with a CoolPix 5700 camera (Nikon Corporation, Tokyo, Japan).

Radioisotope uptake assays

Cells (10^5 per well) were seeded in 12-well tissue culture plates and infected as above. At the indicated time points, culture medium was aspirated, rinsed, and replaced with 10 m*M* HEPES in Hank's Balanced Salt Solution (HBSS) containing 0.1 m*M* NaI and 10^5 cpm of ^{125}I. Control incubations included 0.1 m*M* $KClO_4$ to confirm NIS-specific isotope uptake (data not shown). Cells were incubated for 45 min at 37°C, 5% CO_2, followed by aspiration and rinsing in ice-cold HBSS, then lysed in 1 *M* NaOH for 5 min with shaking. Radioactivity of lysates was measured using a Wizard^2 2470 Automatic Gamma Counter (PerkinElmer, Waltham, MA).

Burst assays

Cells (4×10^6) were plated on 100-mm dishes and infected at MOI 20 of virus, followed 4 hr later by washing and replacement with 10 ml of fresh medium. At 48 and 96 hr post infection, medium was collected and titered by plaque assay on HEK 293A cells.

Animal studies

All experimental protocols were approved by and conducted under guidelines of the Mayo Foundation Institutional Animal Care and Use Committee. All animals were purchased from Harlan Laboratories (Indianapolis, IN) and maintained in the animal barrier facilities of the Mayo Foundation.

Subcutaneous tumor models

Xenografts of the LNCaP and C4-2 cell lines were established by subcutaneous injection of 4×10^6 cells of the respective line suspended in 250 μL of a 1:1 mixture of culture medium and BD Matrigel Basement Membrane (BD Biosciences, Franklin Lakes, NJ) in the right flanks of 4–6-week-old Foxn1nu mice (Harlan). Mice were examined twice weekly for tumor development. LNCaP tumors appeared 4–8 weeks post injection, and C4-2 tumors appeared 2 weeks post injection. Mice were kept on an iodine-deficient diet supplemented with L-thyroxine (5 mg/L) in the drinking water to reduce thyroidal iodine uptake.

In vivo *radioisotope uptake measurement by SPECT-CT*

Mice bearing tumor xenografts of 200–250 mm^3 were injected intratumorally with 10^9 pfu of the viral constructs described above, or left untreated as control ($n=4$ per group). At the given time points (measured in days post viral injection), mice were injected intraperitoneally with 0.5 mCi of ^{99}Tc as sodium pertechnetate. Mice were then anesthetized by induction of 4% isofluorane using a Summit Medical Anesthesia Machine (Summit Medical Equipment Company, Bend, OR), transferred to the examination bed of a Gamma Medica XSPECT System (Gamma Medica, Inc., Northridge, CA), and kept under anesthesia by induction of 2% isofluorane through a nose cone. The SPECT Scan was performed with a parallel-hole collimator, field of view of 12.5 cm, with resolution of 1–2 mm. Sixty-four projections, 10-sec each, were acquired to create a three-dimensional isotope uptake map. The CT scan was performed with a continuous circular orbit 256. Images were acquired at 80 kVp and 0.28 mA, 50-μm slice thickness, 43-μm resolution. Intratumoral radioisotope uptake was quantified using the PMOD Biomedical Image Quantification and Kinetic Modeling Software (PMOD Technologies, Zurich, Switzerland).

Efficacy studies

Mice bearing LNCaP xenografts of $\sim$100 mm^3 were sorted randomly into five groups: one receiving no treatment (control), two receiving an intratumoral injection of 10^9 pfu (3×10^{10} vp) of the indicated vector (virotherapy), and two receiving a viral injection followed by an intraperitoneal injection of 2 mCi of ^{131}I 4 days post infection (radiovirotherapy). For reporting purposes, the day virus was injected was set as day 0. Tumor volumes were measured twice weekly until mice were euthanized due to tumor growth beyond 1,000 mm^3 or ulceration of tumor, as required by our animal use committee. Mice that did not die due to tumor burden were censored, and all surviving mice were euthanized at 100 days post treatment.

Results

In vitro *studies*

In order to characterize the specificity of the CRAds, we first examined both the specificity of virus-mediated cell death and radioisotope uptake. For this, we conducted experiments in three prostatic cell lines: the androgen-dependent LNCaP, its androgen-independent, AR-expressing derivative C4-2 (Gregory *et al*., 2001), and the AR-lacking PC-3 cell line.

Cytopathic effect of Ad5/3PB vectors

MTS assays and crystal violet stains of infected cells showed that both Ad5/3PB-ADP-hNIS and Ad5/3PB-hNIS lysed AR-expressing cell lines (Fig. 1B and C). Inclusion of the ADP increased the speed of cell lysis, reducing the effective dose for cytopathic effect by 10-fold in MTS assays and nearly 100-fold in the LNCaP crystal violet stain. In contrast, the PB promoter-controlled vectors induced little cytopathic effect at high MOI in nonpermissive PC-3 cells. Infections performed alongside these using nonspecific control viruses including wild-type E1 promoters showed no difficulty in lysing PC-3 cells (Supplementary Fig. S1; Supplementary Data are available online at www.liebertpub.com/hum).

Radioisotope uptake in CRAd-infected cells

Figure 2 shows specific radioiodide uptake in AR-expressing cell lines, indicating activation of the MLP and late-stage gene expression. Uptake was inhibited by exposure to $KClO_4$, confirming NIS-mediated concentration of ^{125}I (Supplementary Fig. S2). Peaks of uptake occurred the day prior to cytopathic effect as measured by MTS (Fig. 1B) and fell afterward as cells lysed. Reducing the viral dose delayed the peak uptake as expected. As with the MTS assays, infection of PC-3 cells with nonspecific control vectors induced radioisotope uptake

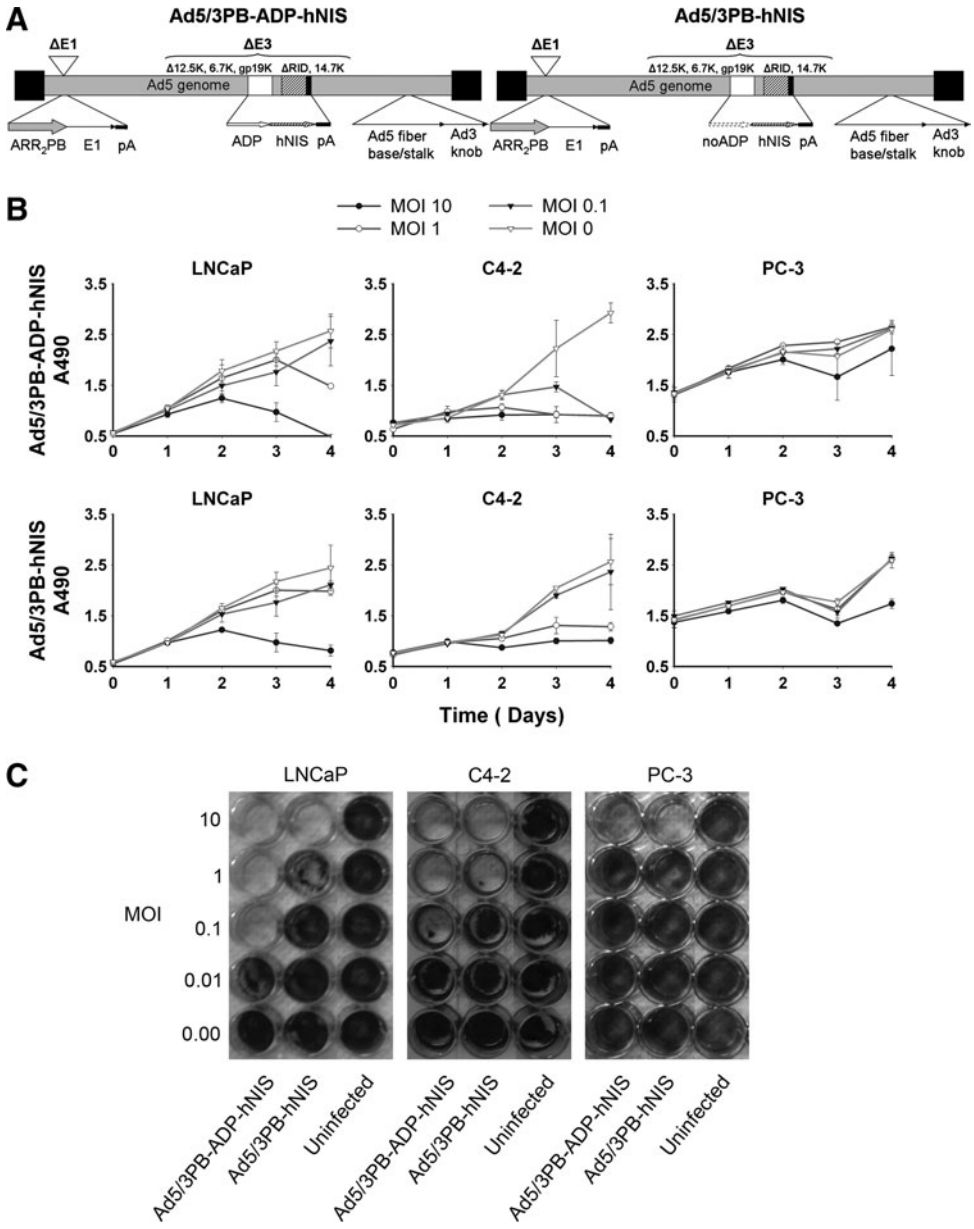

FIG. 1. Structures and cytopathic effect assays. **(A)** Diagrams of the Ad5/3PB-ADP-hNIS and Ad5/3PB-hNIS structures. **(B)** MTS assays: 5,000 cells were infected at the MOIs shown, and absorbance at 490 nm was read in triplicate at each time point. **(C)** Crystal violet stains of cells infected with CRAds at the MOIs shown.

similar to that observed with the CRAds in permissive cells, showing that the PB-promoter E1 control also prevents off-target NIS expression (Supplementary Fig. S3).

In addition, inclusion of the ADP led to distinct phenotypes of iodide uptake. Inclusion of the ADP led to discrete, sharp peaks of uptake, which declined rapidly due to more rapid cell lysis. In contrast, the ADP-lacking vector showed greater uptake in terms of both magnitude and duration. The increased length of uptake with ADP-lacking vector correlated well with the slower rate of viral lysis seen in the MTS and crystal violet assays above. However, at low-dose infection, Ad5/3PB-ADP-hNIS induced uptake more quickly after infection than its ADP-lacking counterpart (Fig. 2B).

Burst assays

Permissive cell lines showed robust viral production 2 days post infection with Ad5/3PB-ADP-hNIS and 4 days post infection with Ad5/3PB-hNIS, resulting in 10^2–10^3 progeny pfu per cell (Fig. 3). By contrast, nonpermissive cell lines produced very weak viral bursts, failing to produce more than one progeny per 10 cells. Although cytotoxicity was observed in cells at 96 hr post infection, this did not result in productive viral replication.

In vivo *SPECT-CT imaging of xenograft tumors*

Mice harboring PCa xenografts were given an intratumoral injection of 10^9 pfu of a viral construct and imaged serially by SPECT-CT (Fig. 4A). Pilot experiments revealed that infected LNCaP and C4-2 xenografts demonstrated robust uptake of ^{99}Tc after infection (data not shown); however, LNCaP tumors were used for long-term imaging and efficacy studies for closer comparison with previous work. Long-term imaging of infected LNCaP xenografts showed uptake well above untreated tumors, nearing ~8–9% of the 0.5-mCi injected dose of isotope at its peak (Fig. 4B). As expected, both Ad5/3PB-ADP-hNIS and Ad5/3PB-hNIS

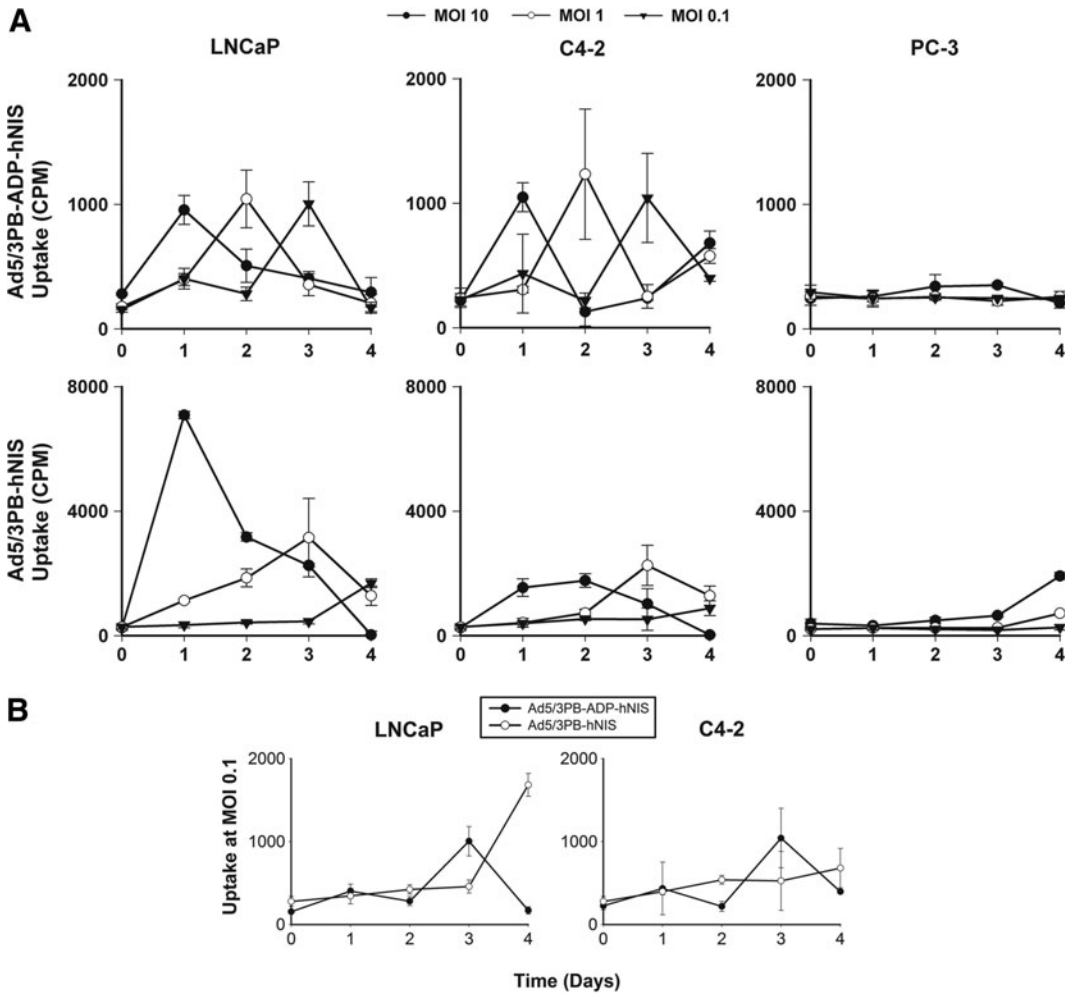

FIG. 2. ^{125}I uptake kinetics. **(A)** Cells (10^5) from permissive and nonpermissive lines were infected with the CRAd vectors and measured daily for radioisotope uptake as described. **(B)** Comparison of uptake in low-dose infection. Cells were infected with either Ad5/3PB-ADP-hNIS or Ad5/3PB-hNIS at MOI 0.1.

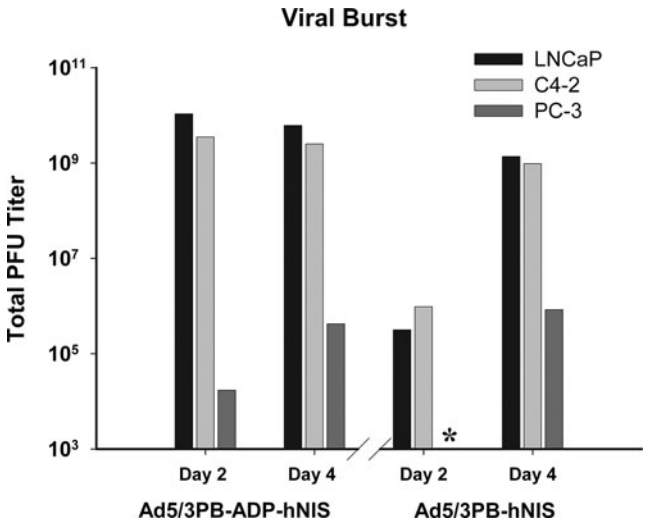

FIG. 3. Burst assay: 4×10^6 of the described cells were infected at MOI 20, and the medium was titered for pfu at 2 and 4 days post infection by plaque assay on HEK 293A cells. *Below detectable threshold of 1,000 pfu.

were outperformed early in infection by Ad5PB-RSV-hNIS, where NIS expression is driven by the strong, nonspecific RSV promoter and is not dependent on viral replication. Later time points revealed increasing uptake induced by Ad5/3PB-ADP-hNIS, consistent with rapid viral replication. These *in vivo* uptake results resemble those seen in the *in vitro* uptake assays at low-dose infection, which resulted in earlier uptake in cells infected with Ad5/3PB-ADP-hNIS.

Efficacy

The potential utility of our CRAd constructs is measured most importantly by their ability to extend the survival of tumor-bearing mice after radiovirotherapy treatment. To test this, we administered 10^9 pfu (3×10^{10} vp) of Ad5/3PB-ADP-hNIS or Ad5/3PB-hNIS via intratumoral injection to ~100-mm^3 LNCaP tumors. Four days later, mice injected with either vector were additionally treated with 2 mCi of ^{131}I ($n=10$ for each group). Mice were then killed when the tumors grew to greater than 1,000 mm^3 or ulcerated, or the mice exhibited other obvious signs of distress. Two mice that died for reasons other than those listed were censored. Untreated LNCaP tumors varied in the onset of logarithmic

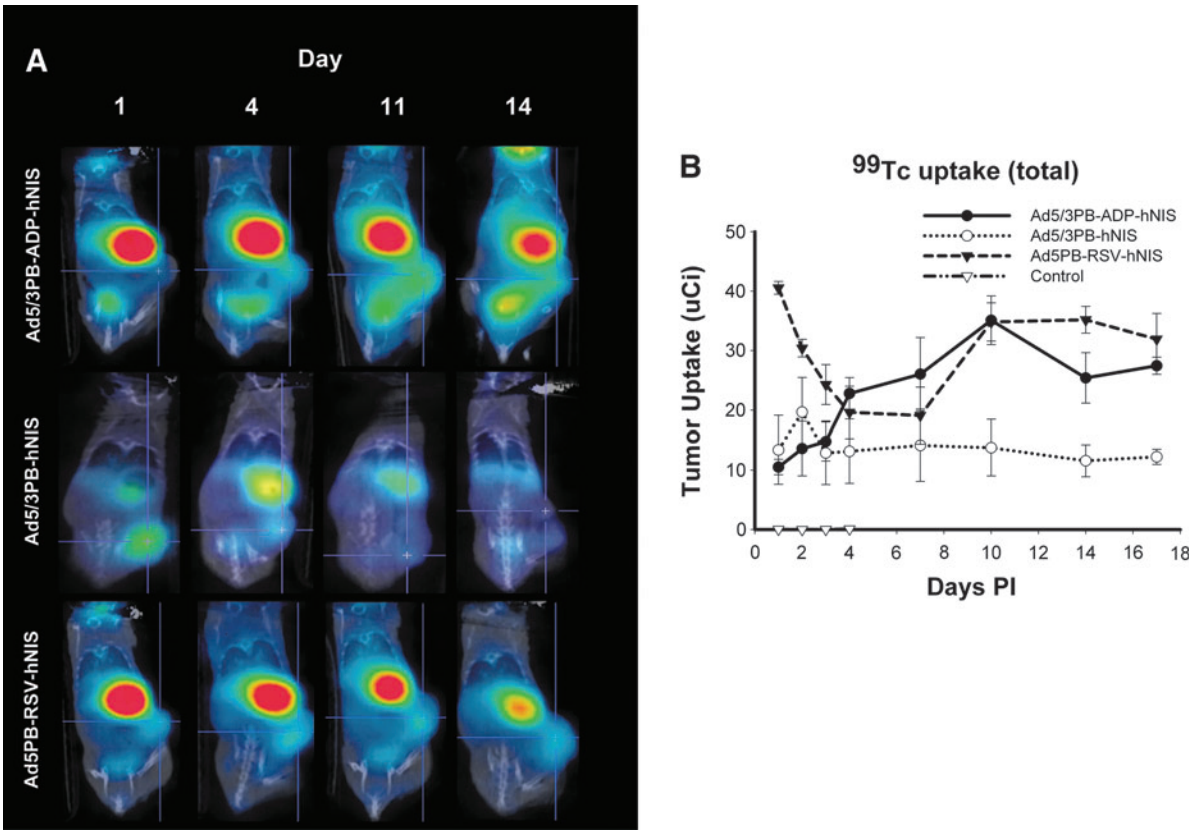

FIG. 4. *In vivo* radioisotope uptake of LNCaP xenografts. Tumor-bearing mice ($n=4$) were imaged at the time points shown after injection of 10^9 pfu of virus. At each time point, mice were injected intraperitoneally with 0.5 mCi of ^{99}Tc and imaged by SPECT-CT 1 hr later. Intratumoral uptake was recorded by volume-of-interest analysis. **(A)** Cross-sectional views of intratumoral isotope concentration. **(B)** Radioisotope uptake kinetics over 3 weeks of imaging. p.i., post infection.

growth, similar to previous work (Trujillo *et al*., 2010), but by 5 weeks 90% of the control mice were killed (Fig. 5A). By contrast, tumor growth curves showed that the growth of tumors was heavily suppressed or reversed by treatment with Ad5/3PB-ADP-hNIS and radioiodide. Treatment with Ad5/3PB-hNIS was only significantly different from control when combined with radioiodide ($p=0.02$). Treatment with Ad5/3PB-ADP-hNIS followed by ^{131}I treatment induced the most profound effect compared with controls, resulting in 40% survival at 100 days post infection ($p<0.001$ vs. control). While providing the most significant survival extension against control tumors, statistically significant survival extension was not observed between Ad5/3PB-ADP-hNIS alone and virus plus iodine ($p=0.108$).

Discussion

We have generated CRAd vectors that combine ^{131}I therapy with conventional virotherapy, a treatment termed radiovirotherapy (Dingli *et al*., 2004). These vectors build upon our previous work with nonreplicating (Kakinuma *et al*., 2003) and conditionally replicating (Trujillo *et al*., 2010) vectors to create more effective means of PCa treatment. Radiovirotherapy improves overall treatment effectiveness through a bystander effect mediated by decay of ^{131}I. Additionally, such multimodal therapies address the problem of heterogeneity within a tumor cell population where mutations often confer resistance to monotherapies (Hanahan and Weinberg, 2011).

Ad5/3PB-ADP-hNIS and Ad5/3PB-hNIS resulted in robust radioiodide uptake and tumor cytolysis in AR-expressing cell lines, including the androgen-resistant PCa line C4-2. This is a critical observation because the majority of androgen-resistant PCas maintain expression of the AR (Holzbeierlein *et al*., 2004; Crnalic *et al*., 2010). Our *in vitro* results with the C4-2 cell line support the usefulness of the PB promoter system in androgen-resistant prostate tumors (Andriani *et al*., 2001). The minimal cytolysis and ^{125}I uptake observed in nonpermissive cells infected with our CRAds suggested that MLP control of NIS results in tumor-specific transgene expression. These constructs reduce the possibility of toxicity from off-target viral infection and radioiodide uptake present in our previous vector (Trujillo *et al*., 2010). Additionally, this makes NIS expression a stronger indicator of viral replication in these vectors. However, cytolysis and induction of NIS expression in PC-3 cells infected with wild-type E1 vectors show the usefulness of the modified fiber protein in binding to CAR-poor cells such as the PC-3 line (Dash *et al*., 2010; Murakami *et al*., 2010).

The inclusion of ADP led to faster *in vitro* cytolysis, affecting radioisotope uptake in important ways. ADP overexpression hastened cell killing and enhanced spread, which resulted in earlier peaks of radioiodide uptake at low MOI. These results agree with those of other groups using transgene

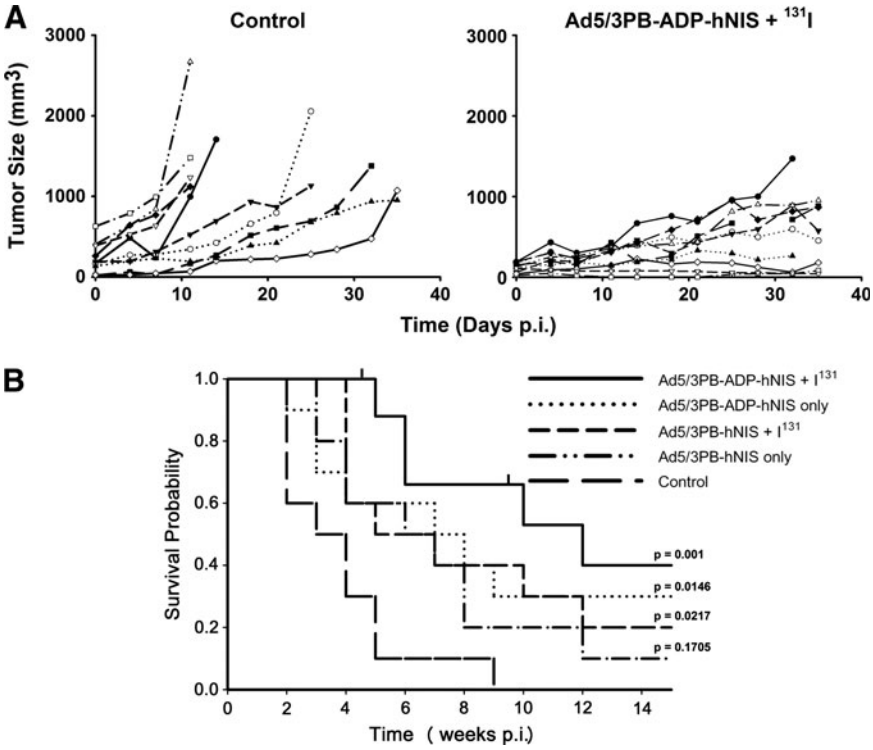

FIG. 5. Efficacy of radiovirotherapy treatment. LNCaP-xenografted mice were injected intratumorally with 10^9 pfu of the CRAd vectors or CRAd injection plus an intraperitoneal injection of 2 mCi of ^{131}I 4 days later ($n = 10$). **(A)** Tumor growth curves comparing mice treated with Ad5/3PB-ADP-hNIS and ^{131}I versus control. **(B)** Kaplan-Meier curves of treated mice. Censored animals are indicated by tick marks. Significance of survival extension was determined by z tests of coefficients and standard errors generated by Cox Proportional Hazard Regression using controls as baseline.

expression as a replication marker of ADP-overexpressing virions (Barton *et al*., 2006; Davydova *et al*., 2010). ADP expression also reduced the peak and duration of uptake at high MOI with Ad5/3PB-ADP-hNIS, because radioiodide concentration requires an intact cell membrane. However, SPECT-CT imaging showed the enhanced spread to be far more important in improving radioisotope uptake *in vivo*.

Our *in vivo* efficacy studies showed that treatment with Ad5/3PB-ADP-hNIS resulted in a significant oncolytic effect. Radiovirotherapy with Ad5/3PB-ADP-hNIS resulted in 40% survival at day 100. Although radiovirotherapy with intratumorally administered Ad5PB-RSV-NIS was equally effective in this model (Trujillo *et al*., 2010), it is an open question whether this vector will be as effective after systemic administration, where issues of low initial transduction and off-target transduction are of much greater concern. The increased specificity of hNIS expression and rate of viral replication observed in Ad5/3PB-ADP-hNIS may improve outcome and should be investigated. In contrast, Ad5/3PB-hNIS showed no significant survival extension as a monotherapy, and minor efficacy against control when combined with radioiodide administration. This indicates that the increased rate of spread seen in AD5/3PB-ADP-hNIS resulted in more viral oncolysis. SPECT-CT imaging at 4 days post infection showed double the radioisotope uptake in AD5/3PB-ADP-hNIS–infected tumors compared with Ad5/3PB-hNIS-infected tumors. Although this indicated that ADP expression improved both radioisotope uptake and viral oncolysis and contributed to survival extension, the benefit of radiovirotherapy compared with virotherapy alone did not reach statistical significance in this model. However, as we consider systemic administration methods where even lower initial transduction rates are observed, these bystander effects may play more important roles in outcome.

In conclusion, Ad5/3PB-ADP-hNIS represents the next step in our development of Ad-NIS vectors for PCa treatment, maintaining efficacy while addressing issues of transgene specificity and inconsistent Ad5 receptor expression on target cells. The results indicate that these vector enhancements improved specificity and therapeutic efficacy of viral oncolysis, and NIS expression in a PCa model.

Acknowledgments

The authors wish to thank Tracy Decklever of the Mayo Nuclear Medicine Animal Imaging Resources for her assistance with SPECT-CT imaging. This work was funded in part by the Minnesota Partnership for Biotechnology and Medical Genomics grant no. 08-06 (J.C.M. and M.Y.), NIH grants R01CA094084 and P50CA101955 project 4 (M.Y.), and the Mayo Prostate SPORE grant P50CA091956 project 3 (J.C.M.).

Author Disclosure Statement

The authors have no conflicts of interest to disclose.

References

Andriani, F., Nan, B., Yu, J., *et al*. (2001). Use of the probasin promoter ARR2PB to express Bax in androgen receptor-positive prostate cancer cells. J. Natl. Cancer Inst. 93, 1314–1324.

Barton, K.N., Paielli, D., Zhang, Y., *et al*. (2006). Second-generation replication-competent oncolytic adenovirus armed with improved suicide genes and ADP gene demonstrates greater efficacy without increased toxicity. Mol. Ther. 13, 347–356.

Barton, K.N., Stricker, H., Brown, S.L., *et al*. (2008). Phase I study of noninvasive imaging of adenovirus-mediated gene expression in the human prostate. Mol. Ther. 16, 1761–1769.

Cho, J.-Y., Xing, S., Liu, X., *et al*. (2000). Expression and activity of human Na^+/I^- symporter in human glioma cells by adenovirus mediated gene therapy. Gene Ther. 7, 740–749.

Crnalic, S., Hörnberg, E., Wikström, P., *et al*. (2010). Nuclear androgen receptor staining in bone metastases is related to a poor outcome in prostate cancer patients. Endocr. Relat. Cancer 17, 885–895.

Dash, R., Dmitriev, I., Su, Z.Z., *et al*. (2010). Enhanced delivery of mda-7/IL-24 using a serotype chimeric adenovirus (Ad.5/3) improves therapeutic efficacy in low CAR prostate cancer cells. Cancer Gene Ther. 17, 447–456.

Davis, B.J. (2011 (ongoing)). Gene therapy and radioactive iodine in treating patients with locally recurrent prostate cancer that did not respond to external-beam radiation therapy. Available at http://clinicaltrials.gov/ct2/show/NCT00788307 (accessed June 22, 2012).

Davydova, J., Le, L.P., Gavrikova, T., *et al*. (2004). Infectivity-enhanced cyclooxygenase-2-based conditionally replicative adenoviruses for esophageal adenocarcinoma treatment. Cancer Res. 64, 4319–4327.

Davydova, J., Gavrikova, T., Brown, E.J., *et al*. (2010). In vivo bioimaging tracks conditionally replicative adenoviral replication and provides an early indication of viral antitumor efficacy. Cancer Sci. 101, 474–481.

Dingli, D., Peng, K.-W., Harvey, M.E., *et al*. (2004). Image-guided radiovirotherapy for multiple myeloma using a recombinant measles virus expressing the thyroidal sodium iodide symporter. Blood 103, 1641–1646.

Doronin, K., Toth, K., Kuppuswamy, M., *et al*. (2003). Overexpression of the ADP (E3-11.6K) protein increases cell lysis and spread of adenovirus. Virology 305, 378–387.

Dwyer, R.M., Bergert, E.R., O'Connor, M.K., *et al*. (2005). In vivo radioiodide imaging and treatment of breast cancer xenografts after MUC1-driven expression of the sodium iodide symporter. Clin. Cancer Res. 11, 1483–1489.

Edwards, J., Krishna, N.S., Grigor, K.M., and Bartlett, J.M.S. (2003). Androgen receptor gene amplification and protein expression in hormone refractory prostate cancer. Br. J. Cancer 89, 552–556.

Galanis, E. (2011 (ongoing)). Recombinant measles virus vaccine therapy and oncolytic virus therapy in treating patients with progressive, recurrent, or refractory ovarian epithelial cancer or primary peritoneal cancer. Available at http://clinicaltrials.gov/ct2/show/NCT00408590 (accessed June 22, 2012).

Gregory, C.W., Johnson, R.T., Mohler, J.L., *et al*. (2001). Androgen receptor stabilization in recurrent prostate cancer is associated with hypersensitivity to low androgen. Cancer Res. 61, 2892–2898.

Hanahan, D., and Weinberg, R.A. (2011). Hallmarks of cancer: the next generation. Cell 144, 646–674.

Holzbeierlein, J., Lal, P., Latulippe, E., *et al*. (2004). Gene expression analysis of human prostate carcinoma during hormonal therapy identifies androgen-responsive genes and mechanisms of therapy resistance. Am. J. Pathol. 164, 217–227.

Hugosson, J., Stranne, J., and Carlsson, S.V. (2011). Radical retropubic prostatectomy: a review of outcomes and side-effects. Acta Oncol. 50, 92–97.

Jemal, A., Bray, F., Center, M.M., *et al*. (2011). Global cancer statistics. CA Cancer J. Clin. 61, 69–90.

Kakinuma, H., Bergert, E.R., Spitzweg, C., *et al*. (2003). Probasin promoter (ARR2PB)-driven, prostate-specific expression of the human sodium iodide symporter (h-NIS) for targeted radioiodine therapy of prostate cancer. Cancer Res. 63, 7840–7844.

Kuster, K., Koschel, A., Rohwer, N., *et al*. (2010). Down-regulation of the coxsackie and adenovirus receptor in cancer cells by hypoxia depends on HIF-1[alpha]. Cancer Gene Ther. 17, 141–146.

Linja, M.J., Savinainen, K.J., Saramäki, O.R., *et al*. (2001). Amplification and overexpression of androgen receptor gene in hormone-refractory prostate cancer. Cancer Res. 61, 3550–3555.

Luster, M., Clarke, S., Dietlein, M., *et al*. (2008). Guidelines for radioiodine therapy of differentiated thyroid cancer. Eur. J. Nucl. Med. Mol. Imaging 35, 1941–1959.

Lutz, P., and Kedinger, C. (1996). Properties of the adenovirus IVa2 gene product, an effector of late-phase-dependent activation of the major late promoter. J. Virol. 70,1396–1405.

Mandell, R.B., Mandell, L.Z., and Link, C.J. (1999). Radioisotope concentrator gene therapy using the sodium/iodide symporter gene. Cancer Res. 59, 661–668.

Mottet, N., Bellmunt, J., Bolla, M., *et al*. (2011). EAU Guidelines on Prostate Cancer. Part II: Treatment of advanced, relapsing, and castration-resistant prostate cancer. Eur. Urol. 59, 572–583.

Murakami, M., Ugai, H., Belousova, N., *et al*. (2010). Chimeric adenoviral vectors incorporating a fiber of human adenovirus 3 efficiently mediate gene transfer into prostate cancer cells. Prostate 70, 362–376.

Ono, H.A., Le, L.P., Davydova, J.G., *et al*. (2005). Noninvasive visualization of adenovirus replication with a fluorescent reporter in the E3 region. Cancer Res. 65, 10154–10158.

Qu, C.F., Li, Y., Song, Y.J., *et al*. (2004). MUC1 expression in primary and metastatic pancreatic cancer cells for in vitro treatment by 213Bi-C595 radioimmunoconjugate. Br. J. Cancer 91, 2086–2093.

Rauen, K.A., Sudilovsky, D., Le, J.L., *et al*. (2002). Expression of the coxsackie adenovirus receptor in normal prostate and in primary and metastatic prostate carcinoma. Cancer Res. 62, 3812–3818.

Scosyrev, E., Messing, E.M., Mohile, S., *et al*. (2011). Prostate cancer in the elderly: frequency of advanced disease at presentation and disease-specific mortality. Cancer 118, 3062–3070.

Spitzweg, C., Dietz, A.B., O'Connor, M.K., *et al*. (2001). In vivo sodium iodide symporter gene therapy of prostate cancer. Gene Ther. 8, 1524–1531.

Tannock, I.F., De Wit, R., Berry, W.R., *et al*. (2004). Docetaxel plus prednisone or mitoxantrone plus prednisone for advanced prostate cancer. N. Engl. J. Med. 351, 1502–1512.

Tollefson, A.E., Ryerse, J.S., Scaria, A., *et al*. (1996). The E3-11.6-kDa adenovirus death protein (ADP) is required for efficient cell death: characterization of cells infected with ADP mutants. Virology 220, 152–162.

Tribouley, C., Lutz, P., Staub, A., and Kedinger, C. (1994). The product of the adenovirus intermediate gene IVa2 is a transcriptional activator of the major late promoter. J. Virol. 68, 4450–4457.

Trojan, L., Schaaf, A., Steidler, A., *et al*. (2005). Identification of metastasis-associated genes in prostate cancer by genetic profiling of human prostate cancer cell lines. Anticancer Res. 25, 183–191.

Trujillo, M., Oneal, M., Davydova, J., *et al*. (2009). Construction of an MUC-1 promoter driven, conditionally replicating adenovirus that expresses the sodium iodide symporter for gene therapy of breast cancer. Breast Cancer Res. 11, R53.

Trujillo, M.A., Oneal, M.J., McDonough, S., *et al*. (2010). A probasin promoter, conditionally replicating adenovirus that

expresses the sodium iodide symporter (NIS) for radiovirotherapy of prostate cancer. Gene Ther. 17, 1325–1332.

Waehler, R., Russell, S.J., and Curiel, D.T. (2007). Engineering targeted viral vectors for gene therapy. Nat. Rev. Genet. 8, 573–587.

Wang, H., Li, Z.-Y., Liu, Y., *et al*. (2011). Desmoglein 2 is a receptor for adenovirus serotypes 3, 7, 11 and 14. Nat. Med. 17, 96–104.

Yamamoto, M., Davydova, J., Wang, M., *et al*. (2003). Infectivity enhanced, cyclooxygenase-2 promoter-based conditionally replicative adenovirus for pancreatic cancer. Gastroenterology 125, 1203–1218.

Zhang, J., Thomas, T.Z., Kasper, S., and Matusik, R.J. (2000). A small composite probasin promoter confers high levels of prostate-specific gene expression through regulation by androgens and glucocorticoids in vitro and in vivo. Endocrinology 141, 4698–4710.

Address correspondence to:
Dr. John C. Morris III
200 1st St. SW
Guggenheim 6-21
Rochester, MN 55904

E-mail: morris.john@mayo.edu

Received for publication March 1, 2012;
accepted after revision May 25, 2012.

Published online: June 13, 2012.